International Journal of Pharmaceutics 381 (2009) 122–129

Contents lists available at ScienceDirect

International Journal of Pharmaceutics

journal homepage: www.elsevier.com/locate/ijpharm

Chitosan–hyaluronic acid nanoparticles loaded with heparin for the treatment of asthma

F.A. Oyarzun-Ampuero [a], J. Brea [b], M.I. Loza [b], D. Torres [a], M.J. Alonso [a,*]

[a] Department of Pharmacy and Pharmaceutical Technology, Faculty of Pharmacy, University of Santiago de Compostela, 15782 Santiago de Compostela, Spain
[b] Department of Pharmacology, Instituto de Farmacia Industrial, Faculty of Pharmacy, University of Santiago de Compostela, Spain

ARTICLE INFO

Article history:
Received 23 December 2008
Received in revised form 23 March 2009
Accepted 8 April 2009
Available online 15 April 2009

Keywords:
Nanoparticles
Chitosan
Hyaluronic acid
Heparin
Asthma
Histamine

ABSTRACT

The purpose of this study was to produce mucoadhesive nanocarriers made from chitosan (CS) and hyaluronic acid (HA), and containing the macromolecular drug heparin, suitable for pulmonary delivery. For the first time, this drug was tested in *ex vivo* experiments performed in mast cells, in order to investigate the potential of the heparin-loaded nanocarriers in antiasthmatic therapy. CS and mixtures of HA with unfractionated or low-molecular-weight heparin (UFH and LMWH, respectively) were combined to form nanoparticles by the ionotropic gelation technique. The resulting nanoparticles loaded with UFH were between 162 and 217 nm in size, and those prepared with LMWH were 152 nm. The zeta potential of the nanoparticle formulations ranged from +28.1 to +34.6 mV, and in selected nanosystems both types of heparin were associated with a high degree of efficiency, which was approximately 70%. The nanosystems were stable in phosphate buffered saline (PBS), pH 7.4, for at least 24 h, and released 10.8% of UFH and 79.7% of LMWH within 12 h of incubation. Confocal microscopy experiments showed that fluorescent heparin-loaded CS–HA nanoparticles were effectively internalized by rat mast cells. *Ex vivo* experiments aimed at evaluating the capacity of heparin to prevent histamine release in rat mast cells indicated that the free or encapsulated drug exhibited the same dose–response behaviour.

1. Introduction

Although mast cells produce a variety of lipid mediators, chemokines, cytokines and enzymes that can interact with airway smooth muscle cells to cause hyperresponsiveness (Page et al., 2001; Robinson, 2004), they are the only endogenous source of heparin in mammals, which plays a protective role by limiting inflammation and airway remodelling (Page, 1991). Heparin is released on degranulation of mast cells (Green et al., 1993) and inhibits the proliferation of smooth muscle cells isolated from the airways of several species including humans (Johnson et al., 1995), bovines (Kilfeather et al., 1995) and dogs (Halayko et al., 1997).

Furthermore, several studies have demonstrated that the inhalation of high, medium and low-molecular-weight heparin (with or without anticoagulant activity) is effective in preventing acute bronchoconstrictor responses and airway hyperresponsiveness, with the potency of these types of heparin being inversely proportional to their molecular weight (Martinez-Salas et al., 1998; Molinari et al., 1998; Campo et al., 1999; Ahmed et al., 2000). This effect was attributed to the capacity of heparin to prevent mast cell degranulation. Interestingly, ultra-low-molecular-weight heparin was also effective in the treatment of late airway responses (pre- or post-antigen challenge); the effect was independent of the anticoagulant activity of the heparin and was mediated by an unknown biological action (Molinari et al., 1998; Ahmed et al., 2000). This is convincing evidence of the potential role of heparin in asthma therapy.

With the aim of enhancing the potential role of heparin in the treatment of asthma, we propose encapsulating this macromolecule in selected nanocarriers capable of positively interacting with mast cells, be internalized by these cells and released the encapsulated heparin in a controlled manner, thereby also preventing the possible degradation of the drug by enzymatic attack in the airways.

CS is a natural, non-toxic, biodegradable polycationic polysaccharide. We, and other groups, have previously used the polymer to elaborate different nanocarriers (Garcia-Fuentes et al., 2005; Köping-Höggård et al., 2005; Prego et al., 2005; De la Fuente et al., 2008a); these nanosystems have been shown, among other advantages, to prolong its residence time at the target site of absorption. These results were mainly attributed to the capacity of the polymer to interact with the negatively charged cell surfaces.

HA is a natural, non-toxic, biodegradable polysaccharide that is distributed widely throughout the human body, mainly in the connective tissue, eyes, intestine and lungs. Several *ex vivo* studies have demonstrated that particulate HA systems have beneficial effects

* Corresponding author. Tel.: +34 981 563100x14885; fax: +34 981 547148.
E-mail address: mariaj.alonso@usc.es (M.J. Alonso).

0378-5173/$ – see front matter © 2009 Elsevier B.V. All rights reserved.
doi:10.1016/j.ijpharm.2009.04.009

on the mucociliary transport rate in airways, due to the mucoadhesivity of the polymer (Prichtard et al., 1996; Lim et al., 2000). It has also been found that HA has a discreet hypoproliferative effect on proliferating airway smooth muscle cells (Kanabar et al., 2005). This may also indicate that HA alone, or in synergy with heparin (Johnson et al., 1995), may be useful in preventing narrowing of the airway in asthmatic patients.

Taking into account this information and the previous experience of our group on the development of CS–HA nanoparticles loaded with hydrophilic and hydrophobic macromolecules (De la Fuente et al., 2008b), the present study aimed to combine the virtues of CS and HA in the development of heparin-loaded nanoparticles, intended for pulmonary administration. Finally, the interaction between these nanosystems and mast cells will be investigated, and their potential for preventing rat mast cell degranulation evaluated, to our knowledge, for the first time.

2. Materials and methods

2.1. Materials

Ultrapure chitosan hydrochloride salt (CS; UP CL 113, molecular weight ~125 kDa and degree of acetylation 14%) was purchased from Pronova Biopolymer AS (Oslo, Norway). Sodium hyaluronate ophthalmic grade (HA, molecular weight ~165 kDa) was a gift from Bioiberica (Barcelona, Spain). Unfractionated heparin sodium salt (UFH, molecular weight ~18 kDa, 202 USP units/mg), low-molecular-weight heparin sodium salt (LMWH, molecular weight ~4 kDa, 53 USP units/mg) and pentasodium tripolyphosphate (TPP) were purchased from Sigma–Aldrich (Madrid, Spain). All other solvents and chemicals were of the highest commercially available grade.

2.2. Preparation of heparin-loaded CS–HA nanoparticles

CS–HA nanoparticles loaded with heparin were prepared according to the procedure previously developed by our group (De la Fuente et al., 2008a). Nanoparticles were spontaneously obtained by ionotropic gelation between the positively charged amino groups of CS and the negatively charged HA, TPP and heparin. Briefly, 3.5 mL of a mixture of an aqueous solution of HA (0.17–0.34 mg/mL), TPP (0.06 mg/mL) and UFH (0.29–0.46 mg/mL) or LMWH (0.4 mg/mL) were added to 3.5 mL of a solution of CS (0.11%, w/v, pH 4.9) under magnetic stirring at room temperature. Magnetic stirring was maintained for 10 min to enable complete stabilization of the system. The nanoparticles were transferred to Eppendorf tubes and isolated by centrifugation in 20 μL of a glycerol bed (16,000 × *g*, 30 min, 25 °C). Supernatants were collected and the nanoparticles were then resuspended in ultrapure water by shaking on a vortex mixer.

The production yield of the systems was obtained by centrifugation of fixed volumes of the nanoparticle suspensions (16,000 × *g*, 30 min, 25 °C), without a glycerol bed. The supernatants were discarded and the sediments were freeze-dried. The yield was calculated as follows:

$$\text{Yield} = \frac{\text{Weight of nanoparticles}}{\text{Total amount of the components}} \times 100$$

2.3. Physicochemical characterization of heparin-loaded CS–HA nanoparticles

The size and zeta potential of the colloidal systems were determined by photon correlation spectroscopy and laser Doppler anemometry, with a Zetasizer Nano-ZS (Malvern Instruments, United Kingdom). Each batch was analyzed in triplicate.

Morphological examination of the nanoparticles was performed by transmission electron microscopy (TEM) (CM12 Philips, Netherlands). The samples were stained with 1% (w/v) phosphotungstic acid for 10 s, immobilized on copper grids with Formvar® and dried overnight for viewing by TEM.

2.4. Association efficiency and drug loading of heparin-loaded CS–HA nanoparticles

The association efficiencies of the selected formulations were determined after isolation of nanoparticles by centrifugation, as described in Section 2.2. The amount of unbound heparin in the supernatant was determined by a colorimetric method (Stachrom® Heparin, Diagnostica Stago, France).

The association efficiency of heparin and the drug loading were calculated as follows:

$$\text{Association efficiency} = \frac{\text{Total amount of drug} - \text{Amount of unbound drug}}{\text{Total amount of drug}} \times 100$$

$$\text{Drug loading} = \frac{\text{Total amount of drug} - \text{Amount of unbound drug}}{\text{Weight of nanoparticles}} \times 100$$

2.5. Stability study of heparin-loaded CS–HA nanoparticles in different media

Selected nanoparticle formulations were prepared and centrifuged in the presence of glycerol. Nanoparticles were tested for their stability taking into account the change in size of nanoparticles and possible precipitations in different media at 37° C, including: Hanks' balanced salt solution (HBSS) at pH 6.4 and 7.4, and phosphate buffered saline (PBS), at pH 7.4 (for composition of these solutions, see below). Nanoparticles were incubated in these media and samples were collected at several time intervals (0, 1, 3, 5, 10 and 24 h), and the size distribution of the nanoparticles was measured by photon correlation spectroscopy.

The composition of HBSS was: 137 mM NaCl, 5.4 mM KCl, 0.25 mM Na_2HPO_4, 0.44 mM KH_2PO_4 and 4.2 mM $NaHCO_3$.

The composition of PBS was: 137 mM NaCl, 2.7 mM KCl, 1.4 mM NaH_2PO_4 and 1.3 mM Na_2HPO_4.

2.6. In vitro heparin release studies from CS–HA nanoparticles

Heparin release studies were performed by incubating 0.1 mg of the selected nanoparticles in 1 mL of PBS (pH 7.4) at 37 °C. The samples were centrifuged at appropriate time intervals (1, 5 and 12 h), and the amount of heparin released was evaluated with the heparin kit described above. The concentration of heparin was quantified and calculated by interpolation from the corresponding standard curve.

2.7. Study of interaction of fluorescent heparin-loaded CS–HA nanoparticles with rat mast cells by confocal microscopy

2.7.1. Fluorescein labelling of CS

Chitosan was labelled with fluorescein following a slight modification of the method described by De Campos et al. (2004). The covalent attachment of fluorescein to CS was by the formation of amide bonds between primary amino groups of the polymer and the carboxylic acid groups of fluorescein. Briefly, 250 mg of CS was dissolved in 25 mL of water, and 10 mg of fluorescein (Sigma–Aldrich, Spain) was dissolved in 1 mL of ethanol. These solutions were then mixed, and

EDAC (1-ethyl-3-(dimethylaminopropyl) carbodiimide hydrochloride) (Sigma–Aldrich, Spain) was added to a final concentration of 0.05 M, to catalyze the formation of amide bonds. The reactive mixture was incubated under permanent magnetic stirring for 12 h in the dark, at room temperature. The resulting conjugate was finally isolated by dialysis for 72 h (cellulose dialysis tubing, pore size 12,400 Da; Sigma–Aldrich, Spain) against demineralised water, and freeze-dried. The pH of fluorescent CS was adjusted to the same value as the raw CS solution (pH 4.9) with HCl, for the preparation of fluorescent nanoparticles.

2.7.2. Preparation of fluorescent heparin-loaded CS–HA nanoparticles

Fluorescent nanoparticles were prepared according to the same procedure described in Section 2.2. The selected mass distribution for the preparation of fluorescent nanoparticles was: 4 mg of fluorescent CS, 0.6 mg of HA, 0.21 mg of TPP and 1.4 mg of UFH.

2.7.3. Confocal laser scanning microscopy study

An aqueous solution (50 μL) containing 0.3 mg of isolated fluorescent UFH-loaded CS–HA nanoparticles was incubated with 450 μL of a suspension of mast cells (10×10^3 cells/100 μL) in Umbreit (for composition, see below) containing 0.05% (w/v) of BSA. The mixture was incubated for 2 h at 37 °C, and the cells were then separated by centrifugation (10 min, 200 × *g*) and discarding the supernatants. Two hundred microliters of Umbreit + BSA solution (at 4 °C) were then added to the cell pellet. The pellet was resuspended and centrifuged again to extract the non-internalized nanoparticles. This procedure was repeated once more. Mast cells were fixed for 5 min in paraformaldehyde (2%, w/v; 100 μL) and washed 3 times with the Umbreit + BSA solution, by centrifugation. Two hundred microliters of a Bodipi® phalloidin solution (Invitrogen, USA) were added to the cell pellet and the cells were incubated for 30 min at room temperature. The cells were washed 3 times (Umbreit + BSA) by centrifugation, the supernatant was discarded, and the pellet was resuspended in 20 μL of the Umbreit + BSA solution. The resuspended sample was placed on the surface of a positively charged microscope slide (Superfrost Ultra Plus, Menzel-Glaser, Ireland) and dried at room temperature overnight. The sample was prepared in Vectashield medium (Vector, USA) for visualization by confocal microscopy (CLSM, Zeiss 501, Germany) (all of the described procedures were carried out in darkness to prevent the loss of the fluorescent signal from the nanoparticles and mast cells).

The composition of Umbreit saline solution was: 1.2 mM $MgSO_4$, 1.2 mM $NaPO_4H_2$, 22.85 mM $NaHCO_3$, 5.94 mM KCl, 1 mM $CaCl_2$, 119 mM NaCl and 0.1% glucose.

2.8. Ex vivo studies with rat mast cells: inhibition of histamine release by heparin-loaded CS–HA nanoparticles

2.8.1. Rat mast cell purification and viability

Mast cells were obtained by lavage of pleural and peritoneal cavities of female Sprague–Dawley rats (400–800 g) with Umbreit saline solution, following procedures similar to those described in other studies (Lago et al., 2001; Buceta et al., 2008). The suspension obtained from each rat was centrifuged at 100 × *g* for 5 min (4 °C) and suspended in a final volume of 1 mL of Umbreit containing 0.05% (w/v) of BSA. Purification was carried by centrifugation on 4 mL of an isotonic Percoll gradient at 600 × *g* for 10 min (4 °C). The mast cells were washed twice with the Umbreit + BSA solution and maintained at 4 °C in this solution until use. Mast cells were quantified by toluidine blue staining (95% purity) and the viability assessed by trypan blue staining (the procedure is described below).

Trypan blue staining procedure: Mast cell viability studies were carried out by trypan blue staining in an inverted microscope, as described by Lago et al. (2001). This involved visual counting of the stained cells in the five fields of a counting chamber. The percentage of viability was calculated with the following formula:

$$\text{Trypan blue stained cells} = \frac{\text{Arithmetic mean from the five fields}}{\text{Total number of mast cells}} \times 100$$

In order to test the mast cell viability after contact with heparin-loaded nanoparticles, the same procedure was used, and the UFH or LMWH-loaded CS–HA nanoparticles added to the rat mast cell suspension (1×10^5 cells per test tube). The tested dose of nanoparticles was equivalent to 200 μg/mL of UFH or LMWH.

2.8.2. Measurement of histamine release in rat mast cells

Rat mast cells (1×10^5 cells per test tube) were pre-warmed at 37 °C (10 min) in BSA-free Umbreit saline solution containing the UFH or LMWH solutions or the nanoparticles loaded with UFH or LMWH. Histamine release from mast cells was then initiated by incubating the cells with 100 μM of compound 48/80 (Sigma–Aldrich, Spain) for 20 min at 37 °C. The cells were then centrifuged at 1100 × *g* for 3 min at 4 °C, and two aliquots (100 μL) of the supernatants were collected in a 96-well microplate. The rest of the supernatants were discarded and the pellets were resuspended in 500 μL of 0.1 mM HCl, sonicated for 1 min and centrifuged at 1100 × *g* for 6 min. Two aliquots of 100 μL of the supernatants were collected for residual histamine determination. Histamine was assayed fluorometrically, as described by Lago et al. (2001); briefly, 80 μL of 1 M NaOH was added to 100 μL of the sample, then 50 μL phthaldialdehyde 0.04% (w/v) was added to each well and plate was incubated for 4 min at 25 °C. After this time, 50 μL of 3 M HCl was added and fluorescence was measured within 20 min, at excitation and emission wavelengths of 360 nm and 465 nm respectively, in a Tecan Ultra Evolution reader (Tecan, Switzerland).

2.8.3. Data analysis for measurement of histamine release in rat mast cells

Results were expressed as percentage of the total histamine released after stimulation with compound 48/80. The results were corrected for spontaneous histamine release in the absence of any chemical and under the same conditions. The equation used for the calculation was $HR = [(S - ER)/(S + P - ER)] \times 100$, where HR is the percentage histamine release; S the supernatant fluorescence; ER the fluorescence of spontaneous release supernatants and P the pellet fluorescence.

IC_{50} values were obtained by fitting the data with non-linear regression, with Prism 2.1 software (GraphPad, San Diego, CA).

2.9. Statistical analysis

The statistical significance of the differences between formulations was determined by application of two-way analysis of variance (ANOVA) followed by a two-tailed paired Student's *t*-test. Differences were considered significant at $p < 0.05$.

3. Results and discussion

3.1. Preparation and characterization of heparin-loaded CS–HA nanoparticles

Nanoparticles loaded with heparin were prepared by the ionotropic gelation technique. The ability of CS to form a gel after contact with polyanions by promoting inter and intramolecular linkages (Calvo et al., 1997) enables the formation of the

Table 1
Physicochemical properties of the nanoparticles prepared with different ratios of CS–HA–TPP–heparin (mean ± S.D., $n = 3$).

Amount (mg) CS–HA–TPP–heparin	Size (nm)	Polydispersity index	Zeta potential (mV)	Appearance
4–1.2–0.21–1.0[a]	201 ± 24	0.22–0.36	+32.1 ± 1.6	Medium turbidity
4–1.2–0.21–1.2[a]	217 ± 30	0.23–0.35	+28.1 ± 0.9	High turbidity
4–1.2–0.21–1.4[a]	Not resuspendable	–	–	–
4–1.2–0.21–1.6[a]	Precipitation	–	–	–
4–0.6–0.21–1.2[a]	162 ± 17	0.11–0.30	+34.6 ± 0.6	Medium turbidity
4–0.6–0.21–1.4[a]	193 ± 32	0.24–0.45	+32.5 ± 1.7	High turbidity
4–0.6–0.21–1.5[a]	Not resuspendable	–	–	–
4–0.6–0.21–1.4[b]*	152 ± 10	0.17–0.27	+33.0 ± 1.3	Low turbidity

[a] UFH
[b] LMWH

Table 2
Loading characteristics and yield of selected CS–HA nanoparticles containing UFH or LMWH (mean ± S.D., $n = 3$).

Amount (mg) CS–HA–TPP–heparin	Loading capacity (%)	Association efficiency (%)	Yield (%)
4–0.6–0.21–1.4[a]	33.6 ± 1.2	72.3 ± 2.7	49.0 ± 1.2
4–0.6–0.21–1.4[b]	60.6 ± 0.3	69.7 ± 7.6	24.9 ± 4.3

[a] UFH
[b] LMWH

nanoparticles. In this case, an ionic interaction occurs between the positively charged CS and the negatively charged HA, heparin and the polyanion TPP. The ionic gelation process is extremely simple and involves mixing two aqueous phases at room temperature.

When the nanoparticles loaded with UFH were prepared, it was necessary to establish the best ratio between components that enabled formation and also adequate isolation of the nanosystems. The size, polydispersity index, zeta potential and appearance of the tested formulations are shown in Table 1. In general, it is possible to argue that when the amount of polyanions was too low (relative to CS), nanoparticles could not be formed, or that the quantity of the formed nanoparticles was too low. Nanoparticles with different characteristics were obtained when greater amounts of polyanions were used. However, if the amount of polyanions was too high, it was impossible to isolate the particles, because the nanosystems were not resuspendable or, in extreme cases, precipitation occurred. In addition, when the amount of polyanions was higher, slight decreases in the positive zeta potential values were observed. This may be caused by increased shielding of free positively charged groups of CS.

All the resulting nanosystems ranged in size from 162 to 217 nm; polydispersity values were between 0.11 and 0.45 and the positive zeta potential ranged from +28.1 to +34.6 (Table 1). This positive zeta potential indicates that the surface of the nanosystems is preferably composed by CS. Among the tested formulations, we selected those formed by the following mass distribution for subsequent studies: 4 mg of CS, 0.6 mg of HA, 0.21 mg of TPP and 1.4 mg of UFH. This formulation was able to encapsulate the highest amount of UFH tested, showed reasonable polydispersity, and high turbidity (related to a higher production yield).

The loading capacity, association efficiency and yield of the selected formulation are shown in Table 2. The association efficiency was 72.3% and therefore 1.01 mg of UFH (of the initial 1.4 mg) formed nanoparticles. The drug loading was about 34%, with the remaining mass corresponding to CS, HA and TPP.

The same formulation prepared with LMWH was similar in size, zeta potential and association efficiency, but showed lower values of polydispersity and yield and higher drug loading (see Tables 1 and 2).

Interestingly, the drug loading of the formulation with LMWH is approximately twice that of the formulation with UFH, and it is possible that LMWH may induce greater displacement of the anionic molecules (HA and TPP) from the nanoparticles and, consequently, lead to a lower yield.

Considering that the only difference between the prepared formulations was the type of heparin, these changes should be attributed, on one hand, to the different molecular weight (~18 kDa for UFH and ~4 kDa for LMWH) and, on the other hand, to possible chemical differences between UFH and LMWH, associated with very different values of anticoagulant activities (202 and 53 USP units/mg, respectively).

The TEM micrographs shown in Fig. 1a and b indicate that the selected nanosystems loaded with UFH or LMWH were spherical.

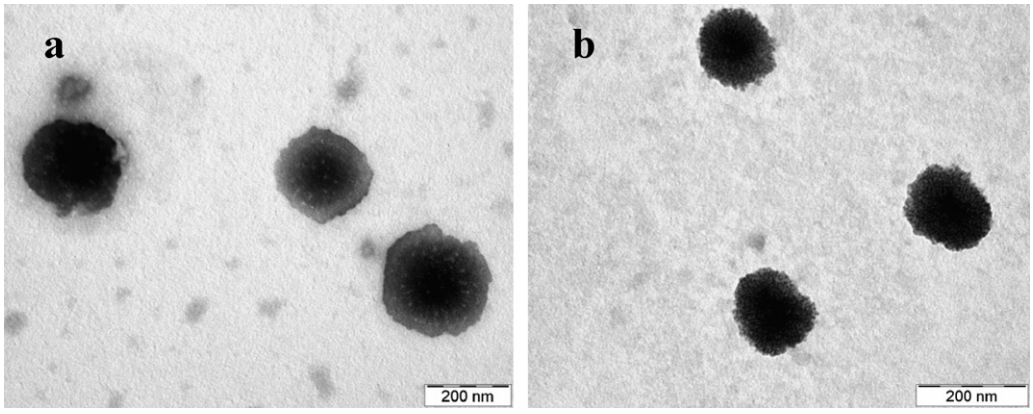

Fig. 1. Electron transmission micrographs of selected CS–HA nanoparticles containing UFH (a) or LMWH (b).

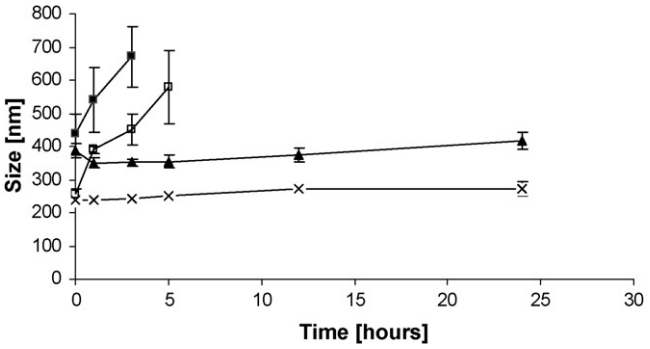

Fig. 2. Stability of heparin-loaded CS–HA nanosystems in different media: UFH-loaded nanoparticles (▲) and LMWH-loaded nanoparticles (×) in PBS (pH 7.4); UFH-loaded nanoparticles (■) and LMWH-loaded nanoparticles (□) in HBSS (pH.7.4) (mean ± S.D., $n = 3$).

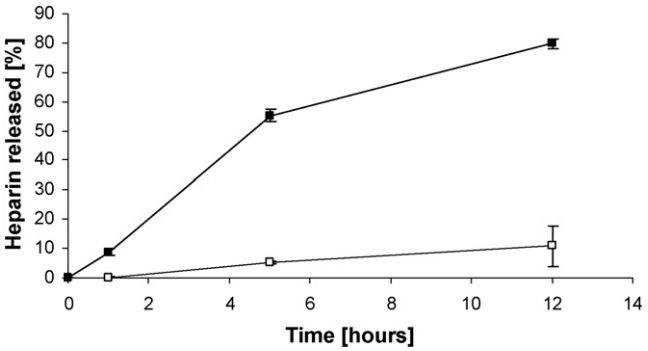

Fig. 3. Heparin release from UFH-loaded CS–HA nanoparticles (□) and LMWH-loaded CS–HA nanoparticles (■) in PBS (pH 7.4) (means ± S.D., $n = 3$).

Interestingly, the systems with UFH appeared denser in the center than at the surface, and differed from those containing LMWH, which appeared more homogeneous.

3.2. Stability studies of heparin-loaded CS–HA nanoparticles

Determination of nanoparticle colloidal stability under conditions similar to those used for cell culture is crucial for future studies. Therefore, the stability of the selected systems was investigated in media usually used for cell culture studies. These media included: HBSS (pH 7.4), HBSS (pH 6.4) and PBS (pH 7.4). The stability of the selected nanoparticles was better in media of pH 7.4, and was maximal for PBS, where the size was maintained for up to 24 h (Fig. 2) (the stability in HBSS (pH 6.4), is not shown because the nanosystems aggregated immediately). The explanation for this difference between PBS (pH 7.4) and HBSS (pH 7.4), may be related to the different composition of these media (HBSS contains CO_3^{2-} ions and a concentration of PO_4^{2-} ions eight times lower than in PBS). This may directly affect the hydration shell of the counterions located at the surface of the nanoparticles, as well as the structure of water surrounding the systems. In PBS these effects appeared to result in an increase in repulsive hydration forces, and hence, greater stability. Interestingly, the zeta values of UFH and LMWH-loaded nanoparticles were slightly negative (-10.5 ± 2 mV) throughout all the stability studies in which HBSS (pH 7.4) and PBS (7.4) were used.

The contact between the nanoparticle formulations with both media produced an increase in size (relative to the corresponding sizes in water, see Table 1). This increase may be related to swelling, attributed to the combination of electrostatic intermolecular repulsion of TPP, HA and heparin (CS chains are partially uncharged at pH 7.4 and the interactions with polyanions become weaker) and the ionic strength of these media, as demonstrated by Lopez-Leon et al. (2005).

The stability of the nanoparticles was also assayed in water at 4 °C, and the nanosystems were stable for up to three months (data not shown).

3.3. Heparin release studies from CS–HA nanoparticles

Taking into account the stability profiles of the selected systems, the release studies were performed in PBS (pH 7.4). The release kinetics of the different heparins was quite different (Fig. 3). In the case of the systems loaded with UFH, the drug was released very slowly, with final release of approximately 10% of the drug within 12 h of incubation. Otherwise, the LMWH was released in a faster, continuous manner, with a final release of approximately 80% in the same period. Considering the high net negative charge of heparin and the positive charge of CS, a strong electrostatic interaction between these oppositely charged macromolecules is expected, resulting in slow drug release. The faster release rate observed for LMWH may be attributed to its smaller molecular weight, which allows better diffusion of the drug from the nanoparticles. There was also an appreciable difference between the drug loading values of the selected systems containing UFH and LMWH (33.6% and 60.6%, respectively). These different values may also affect the release profiles obtained for the two systems.

3.4. Confocal microscopy study of interaction between heparin-loaded CS–HA nanoparticles and rat mast cells

Taking into account that heparin prevents mast cell degranulation via an intracellular receptor (Ahmed et al., 2000; Wong and Koh, 2000; Niven and Argyros, 2003), we aimed to establish whether inclusion of the drug in CS–HA nanoparticles provides intracellular access to the mast cells. Thus, the interaction of fluorescent UFH-loaded CS–HA nanoparticles was observed by confocal microscopy. The overlapping of the fluorescent signal from the incubated nanoparticles (green) with that corresponding to the mast cells (red), resulted in an orange color (Fig. 4.2). This means that the fluorescent nanoparticles effectively interacted with the mast cells after a period of contact of 2 h. We confirmed that this interaction enables the nanoparticles to be internalized in mast cells by observing the fluorescent nanoparticles in sequential slides from the "*z*" axis of mast cells (Fig. 4.3). The positive control (Fig. 4.1) indicates that fluorescent mastocytes did not emit the signal of fluorescent nanoparticles, thus validating the results obtained.

We also tested LMWH-loaded CS–HA nanoparticles, with similar results, but finally selected the systems containing UFH as that they are larger than the former and therefore may be less well internalized by rat mast cells.

3.5. Viability test of mast cells after extraction from rats and contact with UFH or LMWH-loaded nanoparticles

The viability of rat mast cells was higher than 90% in both cases, as assessed by trypan blue staining (see Section 2). The selected dose of UFH or LMWH-loaded nanoparticles to be tested in mast cells corresponded to the highest dose to be administered in the subsequent histamine release studies (equivalent to 200 μg/mL of heparin).

3.6. Ex vivo studies with rat mast cells: inhibition of histamine release by heparin-loaded CS–HA nanoparticles

Considering that heparin-loaded CS–HA nanoparticles were effectively internalized by the mast cells, we decide to evaluate and

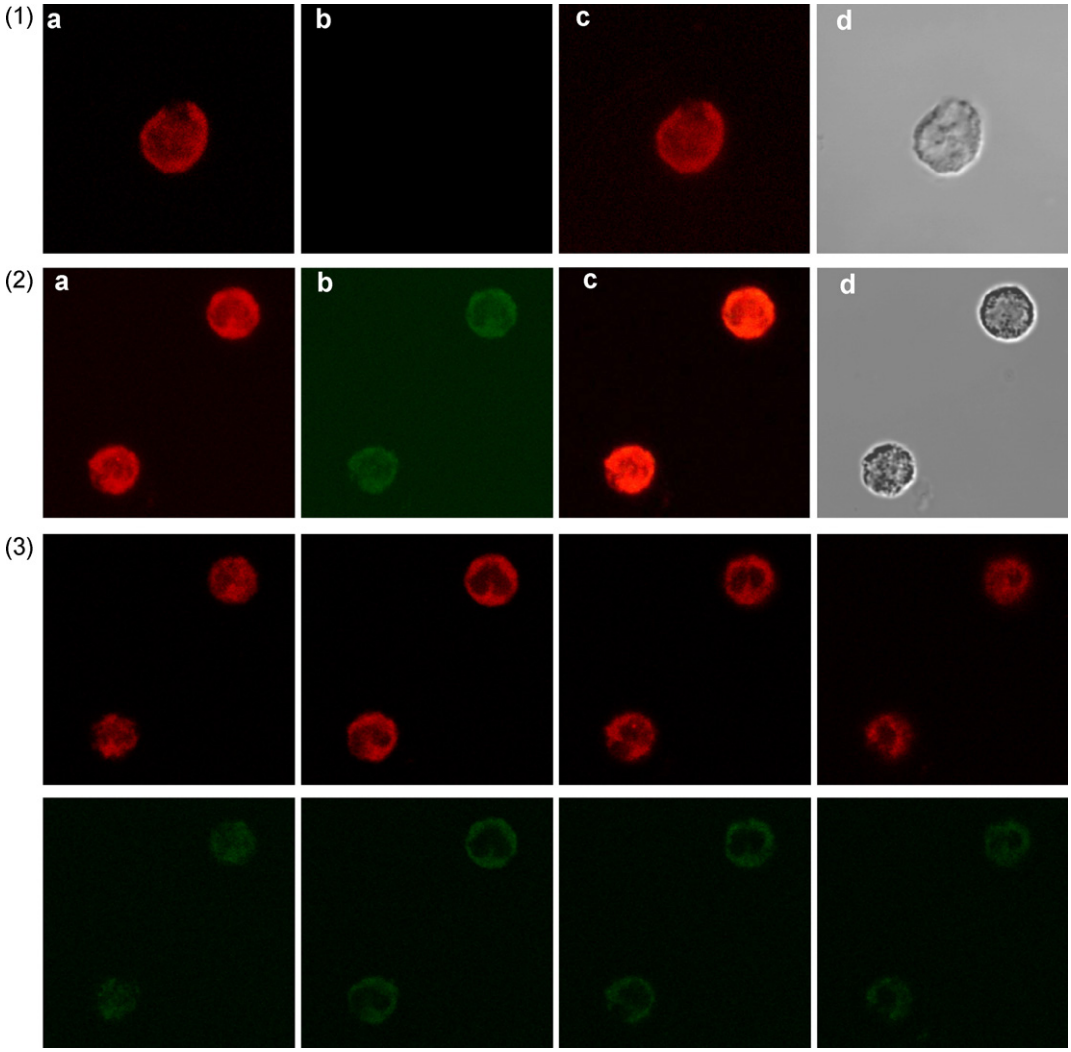

Fig. 4. Confocal laser scanning microscopy images of fluorescent mastocytes and fluorescent UFH-loaded CS–HA nanoparticles. (1) Mastocytes not incubated with nanoparticles (positive control): (a) excitation signal for mastocytes (red); (b) excitation signal for nanoparticles (no signal); (c) overlapping of both signals (red), and (d) optical signal. (2) Mastocytes after incubation with nanoparticles: (a) excitation signal for mastocytes (red); (b) excitation signal for nanoparticles (green); (c) overlapping of both signals (orange), and (d) optical signal. (3) Slides of mastocytes taken every 1.5 μm in the "z" axis, after incubation with nanoparticles. First line: excitation signal for mastocytes (red); second line: excitation signal for nanoparticles (green). (For interpretation of the references to color in this figure legend, the reader is referred to the web version of the article.)

compare the capacity of heparin-administered in the form of solution or loaded in the selected nanoparticles- to prevent histamine release in rat mast cells. To our knowledge, this is the first time that such experiments have been carried out and reported.

Firstly, we tested the effect of different doses of UFH or LMWH in solution on histamine release by rat mast cells; the cells were previously stimulated with a standard substance that elicits degranulation by binding to mast cell granules (compound 48/80) (Ortner and Chignell, 1981). A dose-dependent effect was found, with no significant differences between the different types of heparin (Fig. 5). This confirmed that, under these conditions, heparin was effective at preventing histamine release (IC_{50} (μg/mL) = 6.8 ± 1.2 for UFH and 12.3 ± 3.1 for LMWH), and demonstrated the effective range of concentrations required for this effect.

The effect of the UFH-loaded CS–HA nanoparticles in preventing histamine release, compared with that obtained with UFH solution is shown in Fig. 6a. The dose-dependent effect was maintained, with no significant differences between the UFH solution and the UFH-loaded CS–HA nanoparticles (IC_{50} (μg/mL) = 6.9 ± 1.4 and 3.6 ± 1.8, respectively). Blank nanoparticles did not have any effect on the

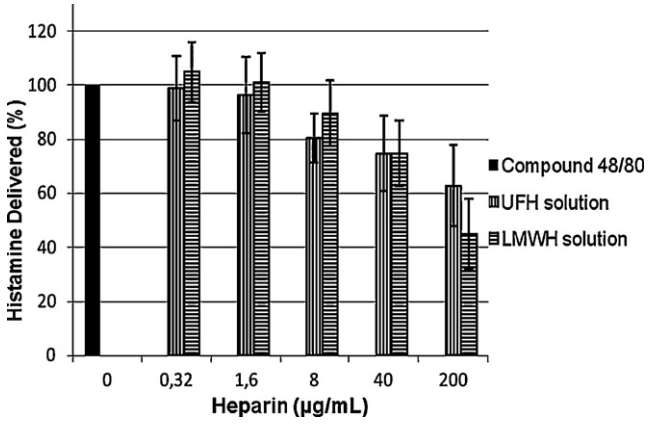

Fig. 5. Effect of UFH and LMWH solutions on histamine-release from rat mast cells. Histamine release was initiated by incubating the cells with a 100 μM solution of compound 48/80 (black bar), and preincubating different concentrations of UFH (vertical-line bars) or LMWH (horizontal-line bars) before the addition of compound 48/80 ($n = 3$, $p < 0.05$).

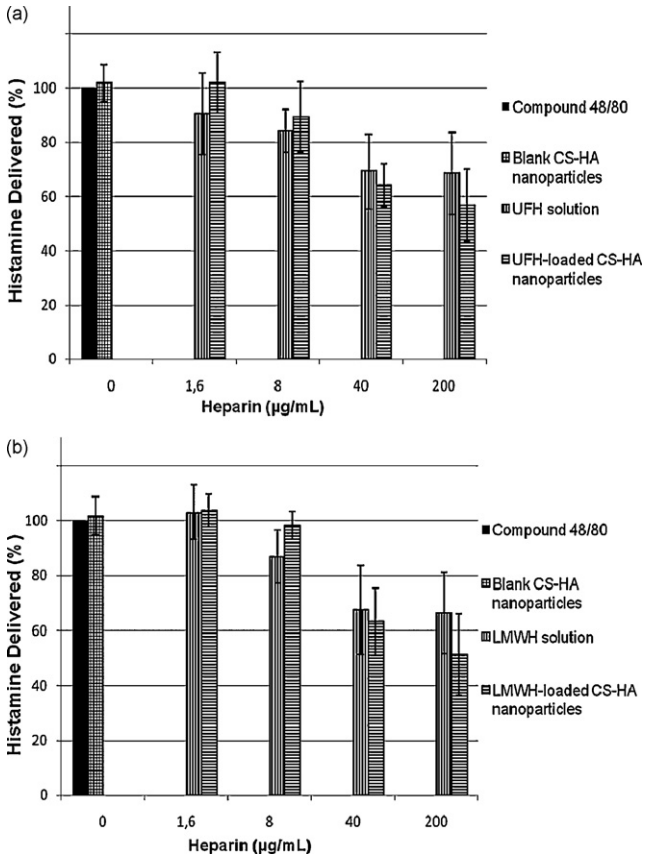

Fig. 6. Effect of heparin solutions and heparin-loaded CS–HA nanoparticles on histamine release from rat mast cells. Histamine release was initiated by incubating the cells with a 100 μM solution of compound 48/80 (black bar) and preincubating different concentrations of (a) UFH solution (vertical-line bars), UFH-loaded CS–HA nanoparticles (horizontal-line bars) or (b) LMWH solution (vertical-line bars), LMWH-loaded CS–HA nanoparticles (horizontal-line bars), before the addition of compound 48/80. As a control, the cells were preincubated with a fixed concentration of blank CS–HA nanoparticles (squared bars) before the addition of compound 48/80 ($n = 3$, $p < 0.05$).

release of histamine from mastocytes (the concentration of the tested blank nanoparticles was chosen according to the highest dose of heparin-loaded nanoparticles tested, thus equivalent to 200 μg/mL of heparin). A similar finding was observed on comparison of the results obtained with the LMWH in solution and LMWH encapsulated in the nanoparticles (IC_{50} (μg/mL) = 5.5 ± 2.1 and 9.6 ± 2.3, respectively) (Fig. 6b).

The results obtained with heparin-loaded nanoparticles are not so promising if they are compared with those obtained with heparin solutions. However, the experimental conditions do not reflect physiological barriers in airways such as mucociliary clearance (via the mucociliary escalator) and enzymatic activity. These barriers may be better overcome by the described polysaccharide nanosystems because of the mucoadhesive-properties of CS (Aspden et al., 1997; Lim et al., 2000) and HA (Prichtard et al., 1996; Lim et al., 2000) and because of the intrinsic capacity of nanoparticles to protect the loaded drug from the enzymatic attack. Additionally, the nanoparticulate formulations may improve the effect of a conventional heparin formulation because of slow drug release, thus prolonging the antiasthmatic effect. Unfortunately, the experimental *ex vivo* conditions do not allow long-term experiments to be carried out.

Whether CS–HA nanoparticles loaded with heparin can really improve the effect of heparin in preventing mast cell degranulation can only be answered by conducting *in vivo* experiments. This is the next challenge in validating our hypothesis.

4. Conclusions

Nanosystems were produced from CS and HA and their suitability as heparin carriers for the treatment of asthma was investigated. Confocal microscopy revealed that heparin-loaded CS–HA nanoparticles were internalized by rat mast cells. However, the capacity of free heparin and of heparin encapsulated in the nanosystems to prevent histamine release was very similar, and showed the same dose–response dependence.

Acknowledgements

The authors acknowledge financial support from the Spanish Government (SAF 2004-08319-C02-01 and Consolider-Ingenio CSD 2006-00012); Felipe Oyarzun-Ampuero was in receipt of a CONICYT scholarship. J.B. received financial support from the Programa Isabel Barreto (Xunta de Galicia). We also thank Mr. Salvador Arines for technical assistance with the mast cells assays.

References

Ahmed, T., Ungo, J., Zhou, M., Campo, C., 2000. Inhibition of allergic late airway responses by inhaled heparin-derived oligosaccharides. J. Appl. Physiol. 88, 1721–1729.

Aspden, T.J., Mason, J.D., Jones, N.S., Lowe, J., Skaugrud, O., Illum, L., 1997. Chitosan as a nasal delivery system: the effect of chitosan solutions on in vitro and in vivo mucociliary transport rates in human turbinates and volunteers. J. Pharm. Sci. 86, 509–513.

Buceta, M., Dominguez, E., Castro, M., Brea, J., Alvarez, D., Barcala, J., Valdes, L., Alvarez-Calderon, P., Dominguez, F., Vidal, B., Diaz, J.L., Miralpeix, M., Beleta, J., Cadavid, M.I., Loza, M.I., 2008. A new chemical tool (C0036E08) supports the role of adenosine A(2B) receptors in mediating human mast cell activation. Biochem. Pharmacol. 76, 912–921.

Calvo, P., Remuñan-Lopez, C., Vila-Jato, J.L., Alonso, M.J., 1997. Novel hydrophilic chitosan–polyethylene oxide nanoparticles as protein carriers. J. Appl. Polymer Sci. 63, 125–132.

Campo, C., Molinari, J.F., Ungo, J., Ahmed, T., 1999. Molecular-weight-dependent effects of nonanticoagulant heparins on allergic airway responses. J. Appl. Physiol. 86, 549–557.

De Campos, A.M., Diebold, Y., Carvalho, E.L., Sanchez, A., Alonso, M.J., 2004. Chitosan nanoparticles as new ocular drug delivery systems: in vitro stability, in vivo fate, and cellular toxicity. Pharm. Res. 21, 803–810.

De la Fuente, M., Seijo, B., Alonso, M.J., 2008a. Bioadhesive hyaluronan–chitosan nanoparticles can transport genes across the ocular mucosa and transfect ocular tissue. Gene Ther. 15, 668–676.

De la Fuente, M., Seijo, B., Alonso, M.J., 2008b. Novel hyaluronan-based nanocarriers for transmucosal delivery of macromolecules. Macromol. Biosci. 8, 441–450.

Garcia-Fuentes, M., Prego, C., Torres, D., Alonso, M.J., 2005. A comparative study of the potential of solid triglyceride nanostructures coated with chitosan or poly(ethylene glycol) as carriers for oral calcitonin delivery. Eur. J. Pharm. Sci. 25, 133–143.

Green, W.F., Konnaris, K., Woolcock, A.J., 1993. Effect of salbutamol, fenoterol, and sodium cromoglicate on the release of heparin from sensitized human lung fragments challenged with *Dermatophagoides pteronyssinus* allergen. Am. J. Respir. Cell Mol. Biol. 8, 518–521.

Halayko, A.J., Recto, E., Sthepens, N.L., 1997. Characterization of molecular determinants of smooth muscle cells heterogeneity. Can. J. Physiol. Pharmacol. 75, 917–919.

Johnson, P.R., Armour, C.L., Carey, D., Black, J.L., 1995. Heparin and PGE2 inhibit DNA synthesis in human airway smooth muscle cells in culture. Am. J. Physiol. 269, L514–L519.

Kanabar, V., Hirst, S.J., OïConnor, B.J., Page, C.P., 2005. Some structural determinants of the antiproproliferative effect of heparin-like molecules on human airway smooth muscle. Br. J. Pharmacol. 146, 370–377.

Kilfeather, S.A., Tagoe, S., Perez, A.C., Okona-Mensa, K., Matin, R., Page, C.P., 1995. Inhibition of serum-induced proliferation of bovine tracheal smooth muscle cells in culture by heparin and related glycosaminoglycans. Br. J. Pharmacol. 114, 1442–1446.

Köping-Höggård, M., Sanchez, A., Alonso, M.J., 2005. Nanoparticles as carriers for nasal vaccine delivery. Exp. Rev. Vaccines 4, 185–196.

Lago, J., Alfonso, A., Vieytes, M.R., Botana, L.M., 2001. Ouabain-induced enhancement of rat mast cells response. Modulation by protein phosphorylation and intracellular pH. Cell Signal 13, 515–524.

Lim, S.T., Martin, G.P., Berry, D.J., Brown, M.B., 2000. Preparation and evaluation of the in vitro drug release properties and mucoadhesion of novel microspheres of hyaluronic acid and chitosan. J. Control. Rel. 66, 281–292.

Lopez-Leon, T., Carvalho, E.L., Seijo, B., Ortega-Vinuesa, J.L., Bastos-Gonzalez, D., 2005. Physicochemical characterization of chitosan nanoparticles: electrokinetic and stability behavior. J. Colloid Interface Sci. 283, 344–351.

Martinez-Salas, J., Mendelssohn, R., Abraham, W.M., Hsiao, B., Ahmed, T., 1998. Inhibition of allergic airway responses by inhaled low-molecular-weight heparins: molecular-weight dependence. J. Appl. Physiol. 84, 222–228.

Molinari, J.F., Campo, C., Shahida, S., Ahmed, T., 1998. Inhibition of antigen-induced airway hyperresponsiveness by ultralow molecular-weight heparin. Am. J. Respir. Crit. Care Med. 157, 887–893.

Niven, A.S., Argyros, G., 2003. Alternate treatments in asthma. Chest 123, 1254–1265.

Ortner, M.J., Chignell, C.F., 1981. The effect of concentration on the binding of compound 48/80 to rat mast cells: a fluorescence microscopy study. Immunopharmacology 3, 187–191.

Page, C.P., 1991. One explanation of the asthma paradox: inhibition of natural anti-inflammatory mechanism by beta 2-agonist. Lancet 337, 717–720.

Page, S., Ammit, A.J., Black, J.L., Armour, C.L., 2001. Human mast cell and airway smooth muscle cell interactions: implications for asthma. Am. J. Physiol. Lung Cell. Mol. Physiol. 281, L1313–L1323.

Prego, C., García, M., Torres, D., Alonso, M.J., 2005. Transmucosal macromolecular drug delivery. J. Control Release 101, 151–162.

Prichtard, K., Lansley, A.B., Martin, G.P., Helliwell, M., Marriot, C., Benedetti, L.M., 1996. Evaluation of the bioadhesive properties of hyaluronan derivates: detachment weight and mucocilliary transport studies. Int. J. Pharm. 129, 137–145.

Robinson, D.S., 2004. The role of the mast cell in asthma: induction of airway hyperresponsiveness by interaction with smooth muscle? J. Allergy Clin. Immunol. 114, 58–65.

Wong, W.S., Koh, D.S., 2000. Advances in immunopharmacology of asthma. Biochem. Pharmacol. 59, 1323–1335.